Environmental Advances 19 (2025) 100616

Contents lists available at ScienceDirect

Environmental Advances

journal homepage: www.sciencedirect.com/journal/environmental-advances

Odor impact assessment in the plume – A validation using tracer gases in two spatial farm configurations

Margret Keck [a,*], Kerstin Zeyer [b], Joachim Mohn [b], Sabine Schrade [c]

[a] Digital Production Research Group, Agroscope, 8356 Ettenhausen, Switzerland
[b] Laboratory for Air Pollution/Environmental Technology, Empa, 8600 Dübendorf, Switzerland
[c] Ruminant Nutrition and Emissions Research Group, Agroscope, 8356 Ettenhausen, Switzerland

ARTICLE INFO

Keywords:
Odor assessment reliability
Odor frequency
Odor intensity
Tracer gas
Longitudinal axis
Livestock husbandry
Biogas plant

ABSTRACT

Livestock facilities and biogas plants pose major challenges for odor assessment due to their spatial extent and the heterogeneity of areal sources. Methods for assessing odor impact in such situations have to overcome points of criticism, such as the lack of reliability and subjectivity in sensory analysis. The aim of this study was to validate an improved procedure for investigating odor plumes by trained assessors. In addition to the widespread approach, which focuses on odor frequency, we combined the odor parameters of intensity and frequency. Due to the relevance of weak and mixed odors, very weak (i.e., perceptible) odors were included, rather than focusing only on recognizable odors (clear, distinct perception). On two farms, a tracer gas approach was implemented to provide an objective measure of dispersion. Comparable spatial patterns in odor parameters (frequency, frequency-weighted odor intensity) and tracer gas concentrations provide a number of key findings to consider in odor assessment of areal sources. Two spatial source configurations were studied—the animal part and the biogas part nested or spatially separated—and discriminated by dosing two different tracer gases. In nested configurations, tracer gases mix homogeneously in the plume and therefore only the combined source can be mapped. By contrast, for spatially separated sources, each position in the plume receives an individual exposure to tracer gases and odor, depending on source arrangement, wind direction, and the adjacent buildings. The presented approach can be extended to reliably track and assign more complex situations. The improved procedures will support objectifying odor impact assessment and pave the way for developing appropriate mitigation strategies.

1. Introduction

Livestock production in Switzerland has undergone enormous changes over the last three decades. In addition to an increase in herd size per farm (Zorn, 2020), more animal-friendly housing implies larger diffuse emitting area sources (Keck et al., 2018a, 2018b). Furthermore, the number of biogas plants in Europe has increased considerably over the last 20 years (Torrijos, 2016). These farms feature an enormous variety of individual odorants and the combined effect of various odor sources from animal husbandry and biogas facilities, such as silage, livestock area, slurry, dung, substrate, fermentation residue storage, and biogas leakage. The impact of odor is mainly determined by (i) the size and arrangement of emitting sources (Keck et al., 2018b), (ii) the mixture of odorants (Hawko et al., 2021), and (iii) the wind conditions and positioning of adjacent buildings, which have a decisive influence on flow and dispersion (Al Jubori, 2016; Aubrun and Leitl, 2004). To elucidate the effect of the spatial source configuration on the impact-side, Schürmann (2007) varied the geometry, homogeneity, and heterogeneity of multiple ground-level areal sources, using inverse dispersion modeling for an airport as an exemplary application. He concluded that the size of the source area controlled the size of the affected area and its uncertainty. Davies et al. (2000) compared how the correlation between the concentrations of two different tracer sources (ammonia and propane) varied with downwind distance, located either side-by-side or longitudinally behind each other. When the sources were separated laterally, the correlation of the two tracer gas concentrations decreased with increasing distance from the sources, whereas when they were separated longitudinally, the correlation increased with distance. However, there is a lack of systematic odor studies for situations with two or more sources and their interaction or source allocation.

Approaches to measuring and predicting odors, with the aim of achieving consistency in odor exposure assessment, range from odor

* Corresponding author.
E-mail address: margret.keck@agroscope.admin.ch (M. Keck).

https://doi.org/10.1016/j.envadv.2025.100616
Received 12 November 2024; Received in revised form 30 January 2025; Accepted 1 February 2025
Available online 2 February 2025

(emission) source testing, odor dispersion modeling, ambient odor monitoring, and setback distance determination (Barclay et al., 2023; Laor et al., 2014). Nevertheless, discrepancies are increasingly evident in that modeling tools using estimated odor emission rates do not reflect undisturbed ground-level observations (Bydder and Demetriou, 2019; Laor et al., 2014). Most models target single-point source emissions, such as stacks with defined flow, while models for passive area or volume sources (e.g., open houses with natural ventilation) are lacking and/or rely on many assumptions, exhibiting high uncertainties (Barclay et al., 2023; Capelli, 2013; Laor et al., 2014). Human sensory analysis is widely applied to assess odors. Odor scientists have emphasized highly dynamic, excellent sensitivity and extraordinary sensory discrimination abilities (Mc Gann, 2017); however, criticisms concern interpersonal and intrapersonal variability, odor-specific differences in perception, individual experience, and the use of precise terminology (Barczak et al., 2018; Hayes et al., 2023; Hummel et al. 2007; Kaeppler and Mueller, 2013; Keller et al., 2012; Laing and Francis, 1989). Therefore, it is necessary to find improved approaches for an objective impact assessment in the field (Hawko et al., 2021; Hayes et al., 2023; Laor et al., 2014).

The impact of odor patterns results from a combination of interacting factors known as FIDOL: frequency, intensity, duration, offensiveness, and location (Freeman and Cudmore, 2002; Nicell, 2009). There are methodological differences in terms of spatial assessor positioning, timing, and the parameters recorded. Two main methods are used to investigate the spatial dispersion of odors in ambient air with trained assessors: the grid method and the plume method (formalized in European Standards). With the grid method, odor is determined at defined intersection points to provide a map of the exposure (EN 16841-1, 2016). By contrast, the dynamic and static plume methods allow for locating the extent of the downwind odor plume from a specific source crossing transects in zigzag form (EN 16841-2, 2016; Van Langenhove and Van Broeck, 2001; VDI 3940-2, 2006) or sampling odor in intersection lines at different distances from the source, respectively. While the grid method requires a long time period with 104 individual measurements spread over a full year (at least half a year), the time requirements for the plume inspection are less extensive and more situation-specific. Depending on the objective of the individual study, different odor parameters can be used. Some authors have focused on the presence or absence of a recognizable odor (yes/no, based on identifying a specific odor type) and have calculated the frequency (EN 16841-2, 2016; Sucker et al., 2008; VDI 3940-2, 2006). Others have considered odor intensity (perceived relative strength of the odor) an integral part of odor impact assessment (Aatamila et al., 2010; Brattoli et al., 2011; Frechen, 2000; Gostelow et al., 2001). Odor intensity is widely assessed using a 7-point-category scale, ranging from 0 (imperceptible) to 6 (extremely strong), with a clear perception and recognition at level 3 (Hawko et al., 2021; VDI 3940-3, 2010), or a simplified 3-point intensity scale that classifies three levels of intensity: no odor, weak but perceptible odor, and recognizable or strong odor (Bydder and Demetriou, 2019). Beyond the challenge of assigning individual odor sources (odor types), agricultural odors are typically complex and dynamic mixtures of multiple odorants. Additive and/or synergistic effects have been reported. However, most of these compounds are below odor and irritation thresholds, thus offering no possibility of identification (Hayes et al., 2023; Laor et al., 2014; Schiffman et al., 2001).

Better applicability of data in statistical models requires modifying the static plume method—that is, synchronous collection of odor decay data with distance along the longitudinal axis (i.e., at the same wind speed and direction). This was realized in our previous investigations by positioning several assessors one after the other in the currently prevailing plume axis: in pig farms 3 assessors (Keck et al., 2005) and in livestock farms combined with biogas plants 6 assessors (Keck et al., 2018b). A more comprehensive representation of odor impact in linear mixed-effect models to identify influencing variables was achieved by combining odor frequency and intensity, a calculation that weighted odor intensity by frequency (Keck et al., 2018b). These two modifications—positioning assessors in the longitudinal axes and combining perceptible odor frequency with intensity—need to be tested for reliability.

To improve the procedure of assessing odor impact in ambient air, systematic studies are required to validate the reliability of odor parameters in plumes and to improve the understanding of odor exposure in different spatial source configurations (Griffiths, 2014; Hayes et al., 2014; Hayes et al., 2023; Laor et al., 2014; Nicell, 2009). The objectives of this study were to (i) validate our modified method for odor plume inspections along the longitudinal axis using tracer gases as an objective measure of dispersion; (ii) compare the odor parameters in terms of the impact, namely odor frequency and odor intensity weighted by frequency, based on perceptible or recognizable odor; and (iii) determine, track, and compare the spatial distribution of the odor plume from two different source configurations—nested or spatially separated sources—using two tracer gases and their ratio.

2. Materials and methods

This study presents a plume odor assessment using tracer gas dosing/analysis as an objective parameter of odor dispersion to evaluate the reliability of the human odor impact assessment method (Fig. 1). The experiment is based on the following issues: (i) the two artificial tracer gases SF_6 and SF_5CF_3 represent two odor emitting areas of a farm, namely the animal husbandry and the biogas facility; (ii) the dispersion of odor and tracer gases follows the same principles; and (iii) tracer concentrations can be measured and analyzed reliably, thus providing an indicator for dispersion and enabling the validation of the odor plume inspection method. The study comprised two farms, each with livestock husbandry and a biogas plant, implying multiple areal odor sources (Fig. 1). Two different spatial source configurations were investigated. In the nested configuration of farm N, the livestock part and the biogas plant were spatially combined, whereas these two parts were spatially separated in farm S. These two spatial source configurations—nested or spatially separated sources—allowed to determine and track the spatial distribution of the tracer gases in the plume and their ratio as a substitute for the indistinguishable odor of two mixed sources. The measurements were carried out one afternoon in August 2011 on farm N with nested sources and in September 2012 on farm S with separated sources as part of a larger project on eight farms (Keck et al., 2018b). Tracer gas dosing/sampling, the odor impact assessment and the recording of the meteorological parameters were determined simultaneously in precise synchronization.

2.1. Description of the measurement sites

Farm N (nested configuration) kept 100 fattening cattle and 20 young cattle on a bedded sloped floor, with solid and perforated exercise areas with natural ventilation, and solid outdoor areas (Fig. 1). The biogas facility was integrated into the farm in a nested configuration and included an open solid substrate store, a slurry storage underneath the perforated floors inside the cattle housing, a 280 m^3 fermenter and a 750 m^3 liquid fermentation-residue store. The emitting areas were 713 m^2 for animal husbandry, 32 m^2 for solid manure storage, and 77 m^2 for substrate storage. Farm S (spatially separated configuration) kept 26 dairy cows in a cubicle housing with solid (outdoor) exercise areas and natural ventilation. The biogas facility was separated from the dairy housing by approximately 45 m. The solid substrate store was enclosed on three sides and roofed. The slurry store under the housing was constructed with concrete cover. The fermenter had a capacity of 700 m^3 and the secondary fermenter was constructed aboveground with a double membrane and a capacity of 1400 m^3. The emitting areas were 420 m^2 for the animal husbandry and 63 m^2 for the substrate storage. The proportion of the biogas plant's emitting areas in relation to the total emitting area of the farm was 9% for farm N and 13% for farm S.

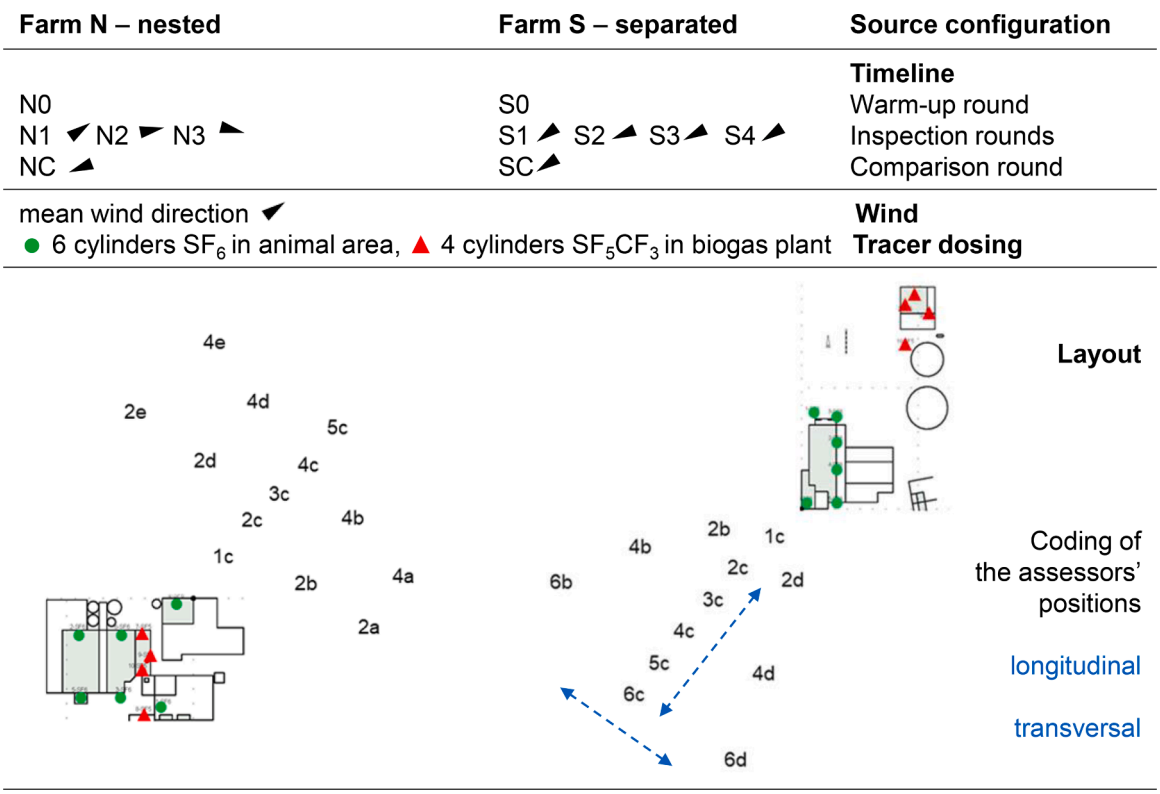

Fig. 1. Layout of farm N with a nested source configuration and farm S with a spatially separated source configuration. *Gray* represents the odor-emitting surfaces, *green dots* depict SF_6 dosing in the animal area, and *red triangles* SF_5CF_3 dosing in the biogas plant. The *black arrows* show the mean wind direction during the individual inspection round. The numbers combined with "*c*" (1*c*–5*c* for farm N, 1*c*–6*c* for farm S) indicate the position of the assessors along the longitudinal axis, and the letters (*a*–*e* for N, *b*–*d* for S) indicate their positions along the transversal axes.

Both farms are located away from other odor-emitting sources in the neighborhood and offer sufficient area and accessibility for plume investigations.

2.2. Tracer gas release, sampling, and analysis

A tracer ratio method with two different tracer gases sulphur hexafluoride SF_6 and trifluoromethyl sulphur pentafluoride SF_5CF_3 was applied over a period of 2 h (Berry et al., 2005; Mohn et al., 2018; Schrade et al., 2012). SF_6 was dosed at the emitting surface areas of the animal husbandry section near the ground, while SF_5CF_3 was used at the biogas facility (Fig. 1). The diluted tracer gases were continuously dosed from six high-pressure cylinders filled with SF_6 (with a concentration of 1.06% on farm N and 1.03% on farm S) and four cylinders filled with SF_5CF_3 (with a concentration of 0.89% on farm N and 0.95% on farm S) in synthetic air (20.5% O_2 in N_2). The tracer gas flow was controlled using critical orifices with a hole diameter of 200 µm (Lenox Laser Inc., MD, USA). The flow rate of the tracer gases was adjusted, applying different pressure settings at the orifice inlet, in response to the actual wind speed to ensure that the analyzed tracer gas concentrations were in an optimal concentration range (>50 ppt, <1500 ppt SF_6 and SF_5CF_3). The flow rates of each critical orifice were monitored before and after each measurement day, and every 15 min during the odor plume inspections (farm N 1.5 L min^{-1} for both tracer gases; farm S 0.7 L min^{-1} SF_6 and 1.5 L min^{-1} SF_5CF_3; GSM, Vögtlin Instruments Inc., Switzerland). Individual orifices agreed within ± 10% (one standard deviation [SD]). The dosing was initiated 30 min before the start of the measurements. On farm N, the total flow of SF_6 from all cylinders added up to 0.63 g min^{-1} and 0.46 g min^{-1} SF_5CF_3, while the flows on farm S were 0.50 g min^{-1} SF_6 and 0.38 g min^{-1} SF_5CF_3. SF_6 impurities in the SF_5CF_3 tracer (1% SF_6 in SF_5CF_3, absolute uncertainty ± 1%), specified by the SF_5CF_3 manufacturer (Fluorochemika, Poland SP.Z00), were corrected but did not affect the study results.

Air samples were collected for 10 min at 13 positions (farm N) and 12 positions (farm S) using 5 L non-permeable gas sampling bags (GSB-P/5, Dr.-Ing. Ritter Apparatebau GmbH & Co. KG, Bochum, Germany). Sampling was conducted using GilAir-5 personal air sampling pumps with a constant low-flow module (Sensidyne, Clearwater, USA). The flow of the pumps was calibrated before and after the survey day. The assessors started and stopped the pumps synchronously with the onset and end of odor inspections.

The tracer gas concentration was quantified in the laboratory using a gas chromatograph (GC, 3400Cx Series, Varian, USA) with an electron capture detector (ECD) according to Berry et al. (2005), Schrade et al. (2012), and Mohn et al. (2018). A correction was applied for background concentration (around 8.5 ppt SF_6, 0.2 ppt SF_5CF_3). Repeatability of gas sampling and GC-ECD analysis was tested with five and three bags, respectively, sampled at the same time and place and resulted in excellent agreements. Repeated gas sampling and GC-ECD analysis in round NC resulted in mean concentrations and coefficients of variation (COV) of 8.7 ppt and 3.4% for SF_6, while the SF_5CF_3 concentration was below the detection limit. At enhanced concentrations (round SC), the mean concentration was 579.2 ppt for SF_6 (COV 1.2%) and 52.5 ppt for SF_5CF_3 (COV 0.9%). In addition, the temporal stability of tracer gas concentrations in the gas bags was demonstrated over 10 days storage (SF_6 ± 0.01 ppt; SF_5CF_3 ± 0.05).

2.3. Odor plume inspections

During the odor plume inspections, each individual assessor was placed in a given single position in the odor plume for 10 min at a time, hereafter referred to as an inspection round (Fig. 1). Three consecutive inspection rounds were conducted on farm N (N1–N3) and four on farm S (S1–S4). The assessors—13 on farm N and 12 on farm S—recorded

their odor perception as intensity for a duration of 10 min for each 10-s interval, resulting in 60 odor perceptions. Women and men were represented among the assessors in almost equal numbers. The scaling of odor intensity followed a 7-level scale from 0 (no odor perceptible) to 6 (extremely strong odor), based on VDI Guideline 3940, Part 3 (2010). Mere odor perception was rated with intensity level 1 (extremely weak, perceptible odor) or level 2 (weak). A distinct odor and the recognition of the odor source were assigned to level 3 (recognizable odor). At the end of each inspection round, the assessors noted the type of odor that they clearly recognized during the round. They also documented any relevant information about their positions. For data input, ASUS P552w PDA handheld PCs with MF3 V2.1 software (ECOMA, Honigsee, Germany) and Psion Series 3a with Olfacto software (ECOMA, Honigsee, Germany) were used. Paper protocols were also used. A visual signal enabled the synchronized start of each round, while an acoustic tone indicated the 10-s intervals.

The first step was to determine the prevailing odor plume using wind vanes or, in the case of a very weak flow, with smoke samples leeward from the emitting source. To cover the spatial extent of the plume, the assessors were positioned along the longitudinal axis (1*c*–5*c* on farm N, coded as N_{long}; 1*c*–6*c* on farm S, coded as S_{long}) one after the other (Fig. 1). This served to focus primarily on the effect of decay with distance rather than on plume width, as plume width depends heavily on the spatial arrangement of the odor sources and the current flow situation. The assessors were positioned on two (2*a*–2*e*, 4*a*–4*e* at farm N) or three (2*b*–2*d*, 4*b*–4*d*, 6*b*–6*d* at farm S) transversal axes. On farm N, positions 1 to 5 were distributed at a distance of 21 to 91 m from the last emitting point of the farm; on farm S, positions 1 to 6 were between 32 and 97 m. The respective positions of the assessors were logged with an R8 GNSS GPS device (Trimble Germany GmbH, Raunheim, Germany) or GPSMAP 60CSx (Garmin, Romsey, United Kingdom). During breaks between the inspection rounds, the assessors stayed outside the odor plume as much as possible to protect their olfactory sense.

To ensure the quality of the odor evaluation by the assessors, the procedure for each survey day was divided into a short introduction, a warm-up (N0, S0), and a comparison round (NC, SC). After theoretically repeating the assigned definitions as a reminder of the introduction, three different odor samples typical of livestock or biogas facilities were presented in bags and jointly evaluated with a view of the odor intensity scale and of the odor source. This was followed by a warm-up with a first inspection round of the day over a period of 10 min with all assessors at the same place and thus with identical odor exposure (N0, S0). For this purpose, a middle position (3*c* for both farms N and S) along the longitudinal axis was selected, with the expectation that both weak and distinct odor perceptions would occur. Immediately afterward, the 60 intervals with the individual ratings and the temporal dynamics were checked together with the assessors to detect the highest intensity levels and intervals without odor perception. This made it possible to adjust the individual assessment for subsequent inspection rounds in advance. After three or four inspection rounds (N1–N3, S1–S4) combined with tracer gas sampling, a dedicated comparison round was conducted with all the assessors at the same location (NC, SC) in position 3*c* (Fig. 1).

2.4. Meteorological conditions

A meteorological station was positioned well exposed at a distance of 150 m to farm N and 300 m to farm S in accordance with WMO (2023) to allow ruling out the effects from buildings, trees, forests, etc., as far as possible. At a height of 10 m, wind speed and wind direction were measured with a USA-1 Scientific 3D ultrasonic anemometer with turbulence extension (Version 4.42t by METEK, Germany), frequency 10 Hz, and average values over 60 s (farm N) or 10 s (farm S). At a height of 2 m, global radiation (FLA613 GS by Ahlborn Mess- und Regelungstechnik GmbH, Germany), air pressure (MSR Electronics GmbH, Switzerland), air temperature, and relative humidity (Rotronic Messgeräte GmbH, Germany) were recorded at intervals of 1 s or 10 s.

The average air temperatures during the inspection rounds on farms N and S were 29.5 and 18.7°C, the relative humidity 42 and 68%, the air pressure 970 and 950 mbar, and the global radiation varied between 627−704 and 202−463 W m^{-2}, respectively. Fig. 2a and 2b show density plots of the wind direction and the wind speed to illustrate the distribution during the individual inspection rounds. On farm N, the mean wind direction shifted from 235° in round N1 to 259° in N2 and 284° in N3. Farm S displayed less variation within and between rounds S1 (54°), S2 (68°), S3 (63°), and S4 (57°). The average wind speed was 1.7 m s^{-1} on farm N (N1 1.9, N2 1.9, N3 1.4 m s^{-1}) and 4.2 m s^{-1} on farm S (S1 4.6, S2 4.1, S3 4.2, S4 4.0 m s^{-1}).

2.5. Data analyses

The statistical analysis was carried out in R v.4.3.3 (R Core Team, 2023). The comparison of all the assessors at the same time and place (position 3*c*, NC, and SC), and thus with the same odor exposure, was carried out by displaying the odor perception with the respective proportion of the intensity levels (I) during the 60 consecutive intervals. In comparison with the mean of the panel, the percentage of perfect agreement and the percentage of deviations from the mean intensity (OI) were calculated. The intraclass correlation coefficient (ICC) was determined to measure the agreement between 13 or 12 assessors in rating intensity levels (I) in 60 intervals each (Koo and Li, 2016). The ICC values were interpreted as follows: greater than 0.75 = 'excellent', 0.60–0.74 = 'good', 0.40–0.59 = 'fair', and <0.4 = 'poor'.

Different odor parameters were calculated for each individual inspection round and assessor by aggregating the results for the individual 10 s intervals (n = 1−60) during the 10-min duration. In addition to the mean odor intensity (OI), the odor frequency was calculated with the intensities perceptible OF (I ≥ 1) and recognizable OF (I ≥ 3):

- OF (I ≥ 1), odor frequency (%), relative share of the odor intensity levels 1−6
- OF (I ≥ 3), odor frequency (%), relative share of the odor intensity levels 3−6

The odor intensity weighted by frequency OIF was calculated as follows, according to Keck et al. (2018b):

- OIF (I ≥ 1), odor intensity with intensity levels 1−6 weighted by frequency

$$OIF\ (I \geq 1) = \frac{n_{I1} \cdot 1 \ + \ n_{I2} \cdot 2 + n_{I3} \cdot 3 \ + \ n_{I4} \cdot 4 + \ n_{I5} \cdot 5 + \ n_{I6} \cdot 6}{\sum n_{I0-I6}}$$

Pearson's correlation coefficient analysis was used for the variables distance, odor parameters, and tracer concentrations on the farm level. In addition, a subset was created with data collected along the longitudinal axis only. A linear mixed-effects model was used to describe the odor intensity weighted by frequency OIF (I ≥ 1) with the whole dataset and data measured along the longitudinal axis (Pinheiro and Bates, 2000). We accounted for the hierarchical data structure of inspection round b_{ij} and farm b_i in the form of nested random effects. The fixed effect for the target variable odor intensity weighted by frequency OIF (I ≥ 1) was the concentration of the tracer gas SF_6 (in ppt). Graphical residual analyses were used to check the models' assumptions. Effects $p < .05$ were considered statistically significant.

3. Results

3.1. Equivalence of the panel during comparison rounds NC and SC

The results of the comparison rounds NC and SC showed good agreement in odor assessment at both low odor levels on farm N and at variable odor levels on farm S. On farm N, 84% of the ratings were no odor (I = 0) because the assessors were positioned divergently to the

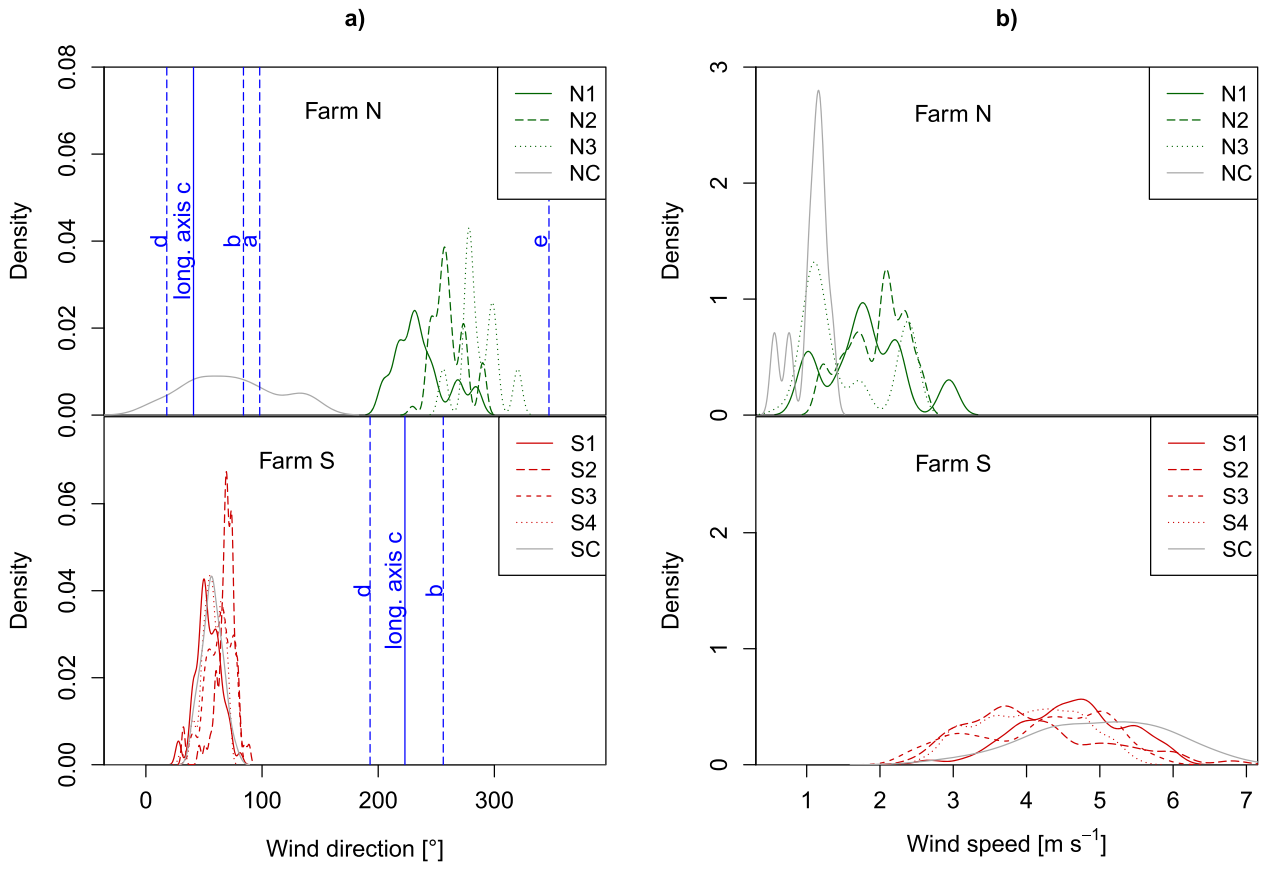

Fig. 2. Density curves of (a) wind direction (degrees) and (b) wind speed (m s^{-1}) during the inspection rounds on farm N (top) and on farm S (bottom), combined with the positions of the longitudinal axes of the assessors on farm N at 41° and on farm S at 223° in *blue color*.

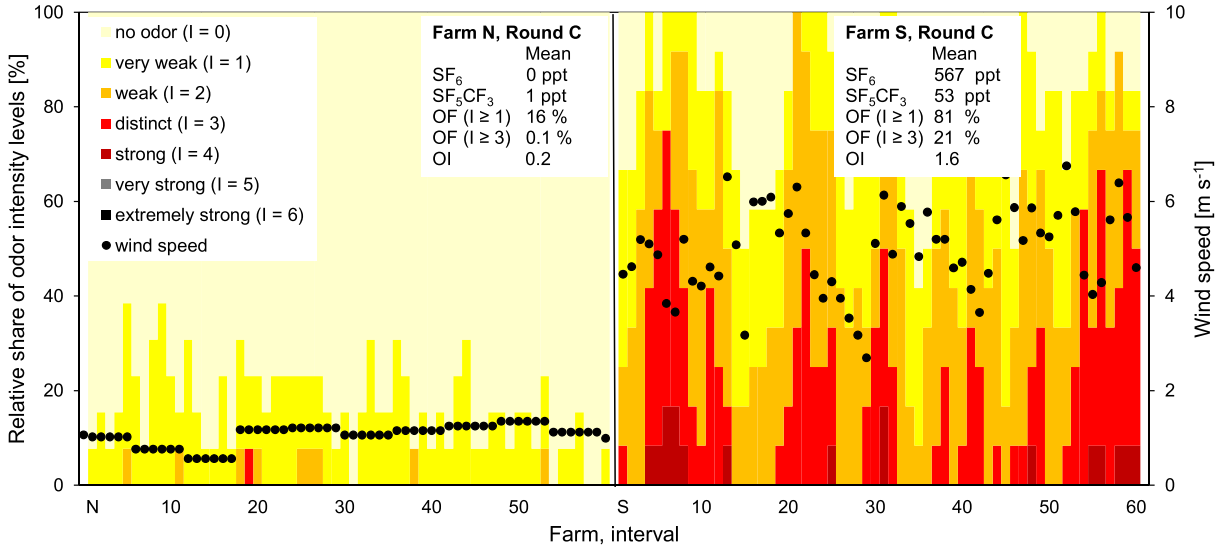

Fig. 3. Relative share of odor perception (%) over time during two comparison rounds, with 60 10-s time intervals, with 13 assessors in inspection round NC and 12 assessors in round SC located at the same place. Odor perception is depicted as intensity levels 0–6 (0 = no odor, 6 = extremely strong odor), supplemented with wind speed in m s^{-1} (*black dots*). The mean tracer gas concentrations (ppt), odor intensity OI, odor frequency OF (I ≥ 1), and OF (I ≥ 3) (%) are provided in a box for the respective comparison round.

wind direction and the effective plume axis. The remainder of the ratings (16%) resulted in very weak (I = 1) or weak (I = 2) odor intensities and thus not assignable to any type of odor (Fig. 3a). On farm S, with a higher wind speed (5 m s^{-1}), odor was observed in 81% of all ratings. The odor intensity varied between level 1 (very weak) and level 4 (strong), with a clear temporal trend in accordance with wind speed (Fig. 3b).

Compared to the panel mean in each interval, on farm N in round NC, 98% of the ratings were identical to the mean of the panel or had a

deviation of one intensity level up. On farm S in round SC, 91% of the ratings were identical to the mean of the panel or had a deviation of one intensity level up or down. This shows a clear synchronous response of the assessors over time and good equivalence in the scaling of the odor intensities. The ICC showed an excellent agreement among the 12 assessors in inspection round SC, using the two-way random effect models and the average rater unit with an ICC value of 0.79 ($p < .001$). In the NC round, the ICC was poor despite the high inter-rater agreement, probably due to the high proportion (84%) of no odor perception (I = 0) and minimal variance. In the immediately preceding introduction and warm-up round N0 (before the start of round N1, with the same panel of assessors and the same position) with a higher odor intensity and frequency, we observed an ICC value of 0.84 ($p < .001$).

3.2. *Intensity and frequency of odor assessments on the longitudinal and transversal axes*

Along the longitudinal axis (central positions *c*), the odor intensity weighted by frequency OIF (I ≥ 1, perceptible odor) (hereafter abbreviated as intensity) and the odor frequency OF (I ≥ 3, recognizable odor) were higher in positions close to the source than in the distant positions (Fig. 4a). Thus, the odor parameters decreased with distance for both

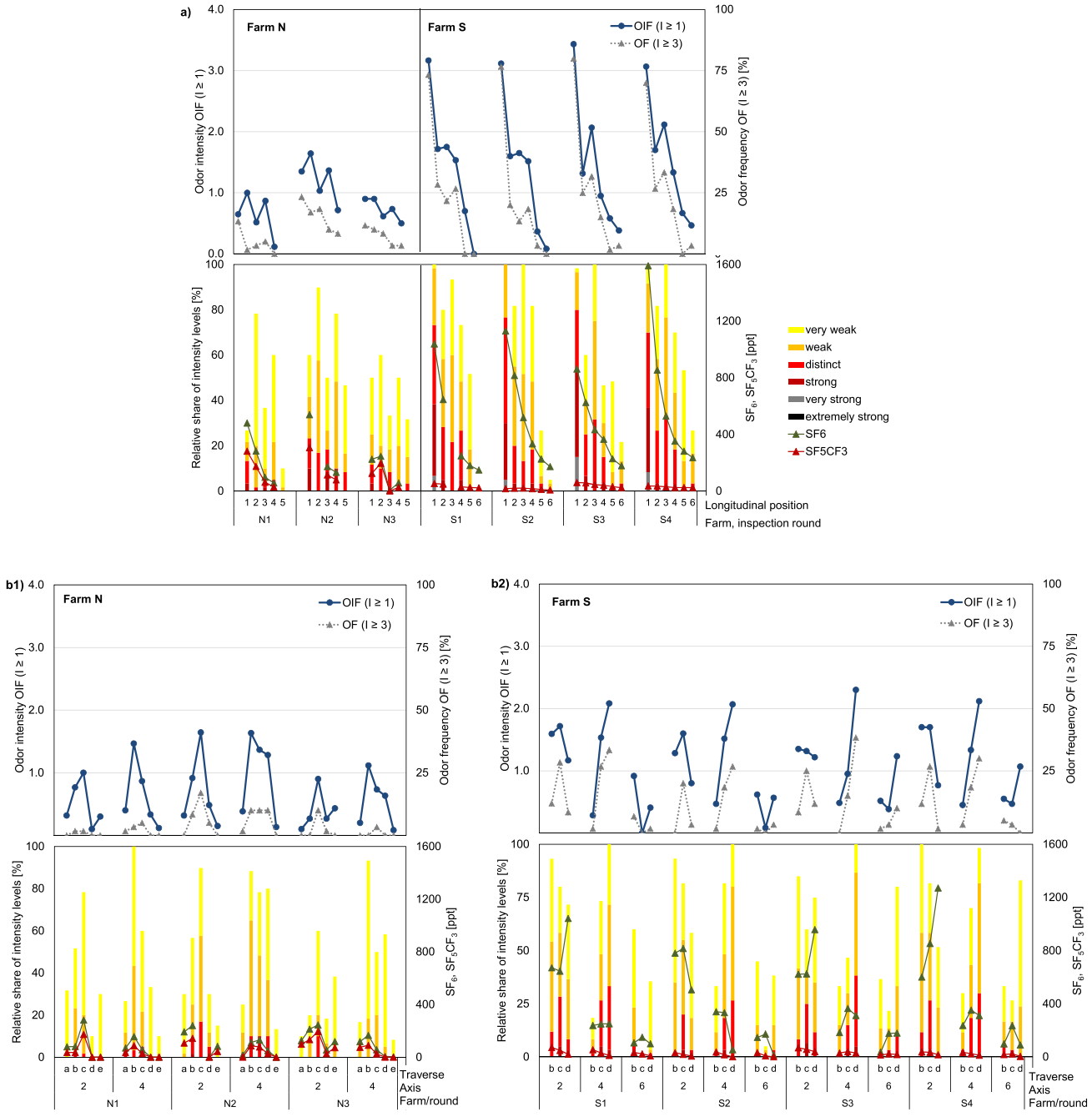

Fig. 4. Relative share of odor perception (%) by the assessors on farms N and S during the inspection rounds N1–N3 and S1–S4 along the longitudinal axis (a), differentiated between the position 1–5/1–6 (1 = close to the farm, 5/6 = far from the farm), and transverse axes on farm N (b1) and farm S (b2), differentiated with respect to positions *a–e/b–d* (*c* = central position). Odor perception is depicted as intensity levels 0–6 (0 = no odor, 6 = extremely strong odor), supplemented by the tracer gas concentrations SF_6 and SF_5CF_3 (ppt), odor intensity with intensity levels 1–6 weighted by frequency OIF (I ≥ 1), and odor frequency, relative share of odor intensity levels 3–6 OF (I ≥ 3), given in %.

farms N and S with OIF (I ≥ 1): 1.6–0.1 and 3.4–0 (maximum–minimum), respectively, and OF (I ≥ 3): 23%–0% and 80%–0%, respectively. Considering all positions, the low intensity levels, very weak and weak (I = 1 and I = 2), were the most common. On farm N, the assessors in positions 1 and 3 rated the odor with lower intensity levels than the assessors in positions 2 and 4 in all 3 rounds, whereas on farm S, the assessor in position 2 was systematically lower than the assessor in position 3. This effect was visible both in the share of intensity levels and in the odor intensity OIF (I ≥ 1). On farm S, an odor frequency OF (I ≥ 1) of 80% or more was mostly found in the three front positions 1–3.

Regarding the odor perception in the two transversal axes (2, 4) of farm N, the middle positions *b, c*, and *d* each had the highest values in terms of odor frequency OF (I ≥ 3) and intensity OIF (I ≥ 1) compared to the outer positions *a* and *e* (Fig. 4b1). On farm S, with three transversal axes (2, 4, 6) and only three assessors within the transversal axis, the difference in odor intensity levels between transversal positions was less consistent (Fig. 4b2). On axis 2, higher values of OIF (I ≥ 1), and OF (I ≥ 3) dominated in the middle position *c*, while OF (I ≥ 1) decreased from positions *b* to *d*. On axis 4, the odor parameters increased in the opposite direction from positions *b* to *d*. On axis 6, the odor parameters were at a lower level, with a smaller gradient between the three positions *b, c*, and *d*.

3.3. Tracer gas concentrations in the longitudinal and transversal axes

The tracer gas concentrations along the longitudinal axis, quantified in the laboratory using a GC-ECD, on farm N decreased from 539 to 6 ppt SF_6 and from 307 to 1 ppt SF_5CF_3, on farm S from 1591 to 148 ppt SF_6 and from 60 to 8 ppt SF_5CF_3 (Fig. 4a). With increasing distance from the sources, a decrease in SF_6 concentration was observed for all inspection rounds, except for round N3, where the SF_6 concentration in the first position was lower than in the second. Similarly, for both farms, the concentration of SF_5CF_3 showed a decay with distance from the farm but at a lower (N) or much lower (S, <60 ppt) concentration level compared to SF_6.

Along the two transverse axes on farm N, the concentrations of SF_6 and SF_5CF_3 were both higher in the middle position of the plume axis (Fig. 4b1). On farm S, the concentration of SF_5CF_3 decreased from position *b* to *d* for all three transverse axes (Fig. 4b2), but a more variable picture emerged for SF_6. At positions further away from the farm (axes 4 and 6), the middle position *c* was usually the highest, but at positions closer to the source, on axis 2, position *d* depicted the highest tracer concentration.

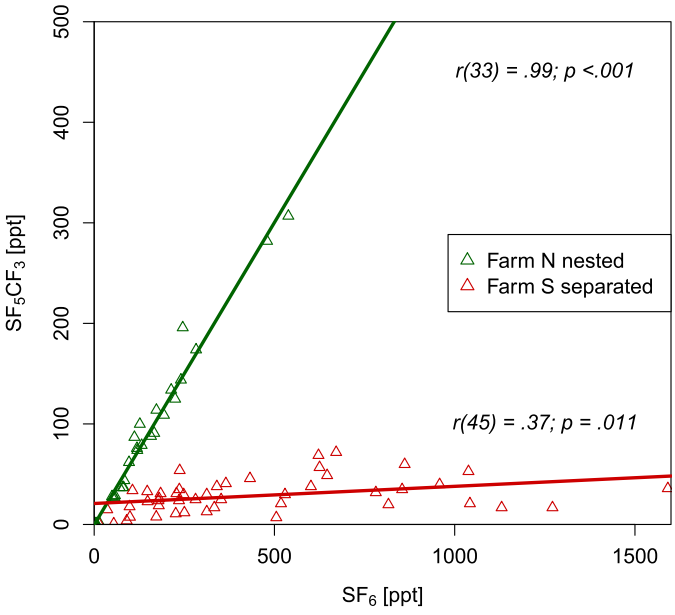

Fig. 5. Correlation of SF_6 and SF_5CF_3 concentrations (ppt) measured at different assessor positions on farm N with nested sources and on farm S with separated sources.

As shown in Fig. 5, the correlation coefficients of the two tracer gases SF_6 and SF_5CF_3 in Table 1 resulted in a significant positive correlation on farm N ($r = 0.99$, $p < .001$) and in a low positive correlation on farm S ($r = 0.37$, $p < .05$). There was a significant negative correlation between distance and both tracer concentrations for all three rounds on farm N (N1–3) with r values of -0.73 ($p < .001$). On farm S, the negative correlation between distance and SF_6 was very high, at -0.88 ($p < .001$), while the correlation for SF_5CF_3 was less strong, at -0.49 ($p < .001$) for all four observation rounds (S1–4) and -0.58 ($p < .01$) for positions along the longitudinal axis only ($S1–4_{long}$).

3.4. Comparison of tracer gases and odor parameters

With increasing distance from the source, the concentrations of the two tracer gases, as well as the odor intensity OIF (I ≥ 1) and the odor frequency OF (I ≥ 3), decreased (Table 1). Considering the data from all inspection rounds and positions on farm N (N1–3), the correlations of colocated SF_6 concentrations and odor perception, that is, OIF (I ≥ 1) (0.44, $p < .01$) and with OF (I ≥ 3) (0.64, $p < .01$), were significant (Table 1). By contrast, the tracer concentration along the longitudinal axis $N1–3_{long}$ showed no significant correlation with OIF (I ≥ 1). On farm S, as shown in Table 1, the highest correlation was observed for the SF_6 tracer gas concentration and OIF (I ≥ 1) and OF (I ≥ 3) both with an *r* of 0.85 ($p < .001$) for measurements conducted along the longitudinal axis ($S1–4_{long}$), while the second tracer gas SF_5CF_3 reached 0.5 ($p < .01$). On farm S, all parameters showed a significant correlation when collected along the longitudinal axis, with the only exception being the two tracer gases (Table 1).

The statistical linear mixed effects models predicted the odor intensity weighted by frequency OIF (I ≥ 1) with the concentration of SF_6, both based on the whole dataset, that is, with all positions of the plume ($p < .001$), and based on the subset along the longitudinal axis ($p < .001$).

3.5. Comparison of nested and spatially separated source configurations

To determine and track the effect of the nested and spatially separated source configurations on the spatial pattern in the odor plume, the observed tracer gas concentration ratios (SF_6/SF_5CF_3) were compared to the ratio of the actually dosed tracers, that is, assuming homogeneous mixing and distribution of both gases. The actual SF_6/SF_5CF_3 ratio was 1.36 on farm N and 1.33 on farm S. On farm N along the longitudinal axis, the observed SF_6/SF_5CF_3 concentration ratios were in the range of the actual ratio of dosed gases, somewhat higher, with values ranging from 1.3 to 2.2, with only a single value in round N3 being substantially higher, at 7.0 (Fig. 6a). These results indicate the homogeneous mixing and distribution of the tracer gases. On farm N with a nested source configuration, no spatial pattern of the concentration ratio SF_6/SF_5CF_3 in the plume was visible in all three inspection rounds; the ratio was of the same order of magnitude at all positions (see Graphical abstract).

On farm S, with spatially separated odor sources, the ratio of tracer gases varied along the longitudinal axis (Fig. 6b) in a very wide range between 6.5 and 67.3, with higher values occurring at positions mainly close to the source where the SF_6 tracer was dosed. Thus, at maximum, the SF_6/SF_5CF_3 concentration ratio was a factor of 50 higher than the actual ratio of the dosed gases. A larger variation in the measured tracer gas concentration ratios was also observed along the transverse axes (Fig. 6c), analogous to the longitudinal axis, with a general trend toward the actual dosed ratio for sampling positions further away from the dosing and in the direction of the remote transversal axis. Consequently, for sampling positions closest to the farm, the odor of the animal husbandry is expected to dominate, while for positions farther away, the

Table 1
Pearson's correlation coefficient *r* with distance, tracer concentrations, and odor intensity weighted by frequency OIF and frequency OF. For each farm, the correlation was calculated for the whole dataset (N1–3, S1–4) as well as based on subsets including only positions along the longitudinal axes (N1–3_{long}, S1–4_{long}). *p*-values indicate the significance level at α = .05 (*$p < .05$, **$p < .01$, ***$p < .001$, H0: ρ = 0, there is no significant linear correlation). Degrees of freedom *df* = n - 2 with SF_6, SF_5CF_3, or distance; odor: N1–3: 33 and 37; N1–3_{long}: 9 and 13; S1–4: 45 and 46; S1–4_{long}: 21 and 22.

Dataset		N1–3		N1–3_{long}		S1–4		S1–4_{long}	
Variable 1	var. 2	*r*	*p-value*	*r*	p-value	*r*	*p-value*	*R*	*p-value*
SF_6	SF_5CF_3	.99	< .001***	.99	< .001***	.37	.011*	.40	.062
Distance	SF_6	-.73	< .001***	-.83	.002**	-.88	< .001***	-.90	< .001***
Distance	SF_5CF_3	-.73	< .001***	-.82	.002**	-.49	< .001***	-.58	.004**
Distance	OIF (I ≥ 1)	-.42	.007**	-.47	.080	-.67	< .001***	-.93	< .001***
Distance	OF (I ≥ 3)	-.60	< .001***	-.61	.015*	-.61	< .001***	-.88	< .001***
SF_6	OIF (I ≥ 1)	.44	.008**	.37	.257	.60	< .001***	.85	< .001***
SF_6	OF (I ≥ 3)	.64	< .001***	.63	.037*	.59	< .001***	.85	< .001***
SF_5CF_3	OIF (I ≥ 1)	.44	.009**	.36	.272	.28	.057	.53	.009**
SF_5CF_3	OF (I ≥ 3)	.64	< .001***	.61	.045*	.27	.064	.52	.010*

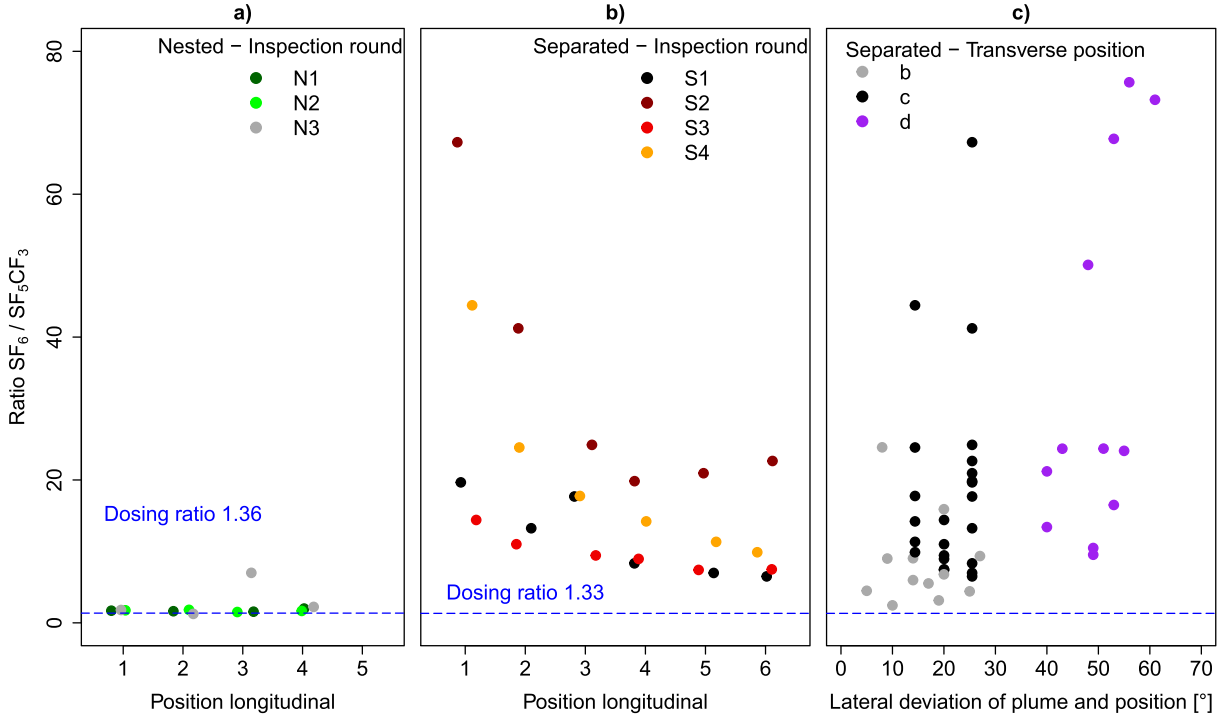

Fig. 6. Observed ratio of SF_6 and SF_5CF_3 concentrations at different sampling positions. In the middle longitudinal axis (a) on farm N with a nested source configuration (positions 1*c*−5*c*), and (b) on farm S with a spatially separated source configuration (positions 1*c*−6*c*) compared to the actual dosing ratio (*blue dashed line*). The individual inspection rounds on farm N (N1–N3) and S (S1–S4) are differentiated by *color*. (c) Lateral deviation (in degrees) between the middle axis of the expected odor plume, based on the mean wind direction, and the position of the individual assessor during the inspection round in relation to the observed ratio of SF_6/SF_5CF_3. The transverse positions (*b*–*d*) are differentiated by color.

relative odor contribution of the biogas plant increased (Figs. 6b). The mean wind direction varied only to a limited extent (54-68°) between the inspection rounds S1−S4. The individual assessors' positions (mainly in axis d, partly in axis c) with a large lateral deviation in degrees from the middle axis of the expected odor plume (Fig. 6c), based on the mean wind direction during each inspection round, showed a ratio of SF_6/SF_5CF_3 concentrations indicating the predominance of the nearby source with animal husbandry. On the other hand, the positions in axis b with a ratio close to the actual dosing ratio indicate the importance of the spatially separated biogas plant (Fig. 6c).

4. Discussion

4.1. Equivalence of the panel during comparison rounds

The assessors' olfactory perceptions during comparison rounds, when assessors were in the same place at the same time, showed good agreement over time (in the course of the intervals) and in the scaling of odor intensities compared to the panel mean at very weak and distinct odor intensities (Fig. 3). Our study included consensus definitions, training, and referencing with typical farm odor samples. On each survey day, a check and comparison of the assessor's intensity scaling was mandatory prior to starting the plume inspections, which also proved valuable in our larger-scale study (Keck et al., 2018b). Gotow et al. (2018) confirmed the value of a warm-up with samples on the performance of assessors in time-intensive evaluations. Whereas Zhang and Zhou (2020) used an 8-point intensity scale realized by n-butanol and pig manure simulants, we used real air samples from farms collected in Nalophan bags to train the odor intensity rating of assessors. In this way, our assessors were already familiar with the odors relevant to the study, in line with Hayes et al.'s (2023) recommendation. The limitations of the current practice of using n-butanol as a reference for overall olfactory

performance with regard to specific odors and mixed odors have also been elucidated in other studies (Barczak et al. 2018; Hayes et al., 2017; Hove et al., 2016; Kaeppler and Mueller, 2013; Laor et al., 2014).

The two very different odor exposures during comparison rounds on the two farms were evident in all odor parameters, for example, the mean value of the odor intensity OI and in the odor frequencies OF ($I \geq 1$) and OF ($I \geq 3$) (Fig. 3). Consistent with the odor parameters, the mean tracer gas concentrations displayed a distinct difference between farms N and S with 0 and 567 ppt SF_6 and 1 and 53 ppt SF_5CF_3, respectively. The percentage of perceptible odor detection on farms N and S, with OF ($I \geq 3$) being 0 (NC) and 21% (SC), was much lower than of recognizable odor, OF ($I \geq 1$) with 16 (NC) and 81% (SC). Reliable identification of the odor—what it smells like—in the plume is more demanding and increases the risk of bias between assessors, especially at high temporal resolution and for mixed odors (Hayes et al., 2023; Hawko et al., 2021; Kaeppler and Mueller, 2013; Laing and Francis, 1989). A better recognition of odors would require much more complex training in advance to clearly identify different odor sources, yet in many field studies, the specific odor sources are not even known in advance. Since weak odor and odor mixtures account for a relevant proportion of time, focusing only on distinct recognizable odors does not seem sufficient for meaningful odor assessments.

4.2. Comparison of spatial patterns of odor parameters and tracer gases

A clear decay with distance from the farm along the longitudinal axis was visible for both tracer gases as well as for the odor parameters on both farms (Fig. 4a). A similar decay of odor intensity was demonstrated in our earlier field studies with cattle, pig farming, and the combination of animal husbandry with biogas facilities (Keck and Frei, 2016; Keck et al. 2005; Keck et al., 2018b). Bydder and Demetriou (2019), as well as Zhang and Zhou (2020), confirmed a decay with distance with a large dataset of field-odor assessments in the case of waste handling facilities or pig farms but at much larger dimensions up to 4000 m distance.

Bächlin et al. (2002) investigated a forced-ventilated pig house in a simplified situation with only one exhaust stack and found correlation coefficients between the tracer gas concentration and odor intensity in a wide range between -0.1 and 0.8 but mostly between 0.6 and 0.8. In our study, the correlation coefficients between tracer concentrations and odor parameters along the longitudinal axis were between 0.36 and 0.85 (Table 1). The lower correlation in the longitudinal axis on farm N could be due to a lower odor intensity, a higher variation in wind direction, or a smaller number of available samples. Including data from the transversal axes, decay with distance was also evident for both tracer gases (Fig. 4b1). On farm S, however, with only three assessor positions in the transversal axis (Fig. 4b2), the two tracer gases and the odor parameters were not always equally aligned. One of the challenges might be the use of the odor parameter frequency OF ($I \geq 1$), as this parameter does not allow sufficient differentiation in cases of a high percentage with odor perception. This is also confirmed by Hartmann and Grabowski (2011), who recommend the use of the parameter odor intensity. By contrast, OF ($I \geq 3$) and OIF ($I \geq 3$) are not appropriate for situations with weak odor exposure (see Section 4.1). The illustrations of the relative proportions of the individual odor intensities along the longitudinal axis as a bar graph (Fig. 4a) are indicative of an interpersonal effect with a zigzag shape, which can only be overcome with training, monitoring, stronger selection, randomization, or sufficient assessors. A practical approach to coping with this challenge could be a more targeted selection of the assessors immediately after the warm-up on each study day. Similarly, Bächlin et al. (2002) reported deviations in odor perception that were attributed to interpersonal effects or limits in the informative value of the parameter odor frequency in cases of very weak odor intensities.

The entire odor situation cannot be fully described if only recognizable odors ($I \geq 3$) are recorded, especially with different source types. Extremely weak and weak odors are missed, and mixed odor recognition is not always possible. With our approach using two tracer gases on farm S, it is obvious that with separate sources and correspondingly separate tracer dosing, complete agreement could not be achieved with a single tracer. This would require two additive tracer gases. Section 4.3 offers more detail on the source configurations, wind direction, and odor impact, with a discussion of a broader context.

4.3. Odor assessment potential for nested and spatially separated source configurations

For farm N with nested sources, a significant correlation of 0.99 ($p < .001$) was observed between concentrations of the two tracer gases, SF_6 and SF_5CF_3, for the different assessor positions, indicating that the entire combined source configuration can be accurately mapped with just one tracer gas (Fig. 5, Table 1). This means that the nested sources cannot be distinguished because they are perceived as one odor source. The largely similar ratio of the concentrations of the two tracer gases SF_6/SF_5CF_3 along the longitudinal axes of farm N between 1.3 and 2.2 indicates homogeneous mixing of the emitted gases and a comparable dispersion of the two tracer sources (see Graphical abstract, Fig. 6a). Since the observed tracer gas ratio was equal to or greater than the actual ratio of the dosed gases of 1.36, the relative impact of SF_6, that is, animal husbandry, under the study conditions was overrepresented relative to SF_5CF_3 representing the impact of the biogas plant.

On farm S with two spatially separated odor and tracer sources, the ratio of tracer concentrations varied both with distance from the source and with sampling point, illustrating a more complex interplay of source configuration, wind direction, and individual position in the plume (Graphical abstract, Figs. 4a, 4b2 and 6b and 6c). The decrease in concentrations with distance from the farm was visible for both tracer gases, even though SF_5CF_3 was at a much lower level (less than 60 ppt). Due to the spatial separation between the two emitting parts within the facility, with a maximum distance of 108 m, tracer and odor emissions from the more distant biogas plant were already diluted prior to being mixed with emissions from animal husbandry. Nonetheless, along the longitudinal axis, the concentrations of both tracer gases SF_6 resp. SF_5CF_3, correlated with the odor parameters OIF ($I \geq 1$) and OF ($I \geq 3$), with correlation coefficients of 0.85 ($p < .001$) and 0.53 ($p < .01$; Table 1), respectively. The ratios between the two tracer gases SF_6/SF_5CF_3 were highest at the positions closer to the source, indicating that tracer/odor perception at these positions was dominated by emissions from the spatially close SF_6 dosing/husbandry buildings (Fig. 6b). The spatial pattern of the two tracer gases in the plume and their ratios at the different assessor positions can be interpreted as a different contribution of the two spatially separated emission sources to the indistinguishable mixed odor.

The positions of the assessors along the longitudinal axis of the plume (angle of 223°, measured from the last emitting point of the animal husbandry, Fig. 1) covered the animal husbandry and the SF_6 dosing points and, consistent with the mean wind direction between 54 and 68° (Fig. 2a), ensured an expected maximum exposure along the middle longitudinal axis between 234 and 248°. This is also reflected in the high correlation coefficients of SF_6 to the odor parameters of 0.85 ($p < .001$, Table 1). If the longitudinal axis is plotted based on the wind direction starting from the last emitting point of the biogas plant and SF_5CF_3 dosing, it becomes obvious that the area affected by the biogas plant and SF_5CF_3 dosing was only marginally covered by the actually selected positions of the assessors, which is also represented by the lower correlation coefficient (0.53, $p < .01$, Table 1). Whereas in round S2, the greatest deviation of the mean wind direction with 69° was visible in the high ratio of the concentrations of the two tracer gases SF_6/SF_5CF_3 in the front positions of the longitudinal axis, the ratio was lower in round S1, with a smaller deviation (54°, Fig. 6b). This effect close to the buildings could be explained by the flow around the buildings and the wake (Aubrun and Leitl, 2004). Furthermore, Eckhof et al. (2012), Moldenhauer et al. (1999), and Olesen et al. (2005) stated that spatially extended sources and building arrangements have a greater bearing on odor impact, and hence on the importance at a particular impact

location, than do smaller-scale, that is, point sources. In our setup with two defined tracer gases and simplified with two somewhat separated odor sources, we found that each position in the plume experienced an individual exposure, which resulted from the interaction of the source arrangement, the respective wind flow, the adjacent buildings, and the respective individual position in the plume. How spatial configurations of spatially extended, heterogeneous sources—with an enormous variety of individual odor sources within and correspondingly different odor release processes—affect odor impact in the vicinity should be investigated in even more detail in future studies.

The wind direction, the source configuration and the flow characteristics of the two dosing areas are decisive for the spatial dispersion/mixing of the tracer gases, and this is also to be expected for the various odor sources. Spatial differences in tracer and odor dispersion became obvious when comparing individual positions in the plume. Accordingly, the contribution of SF_5CF_3 emitted from the biogas plant, relative to SF_6, was highest for positions on axis *b*, while on axis *c* and especially on axis *d*, the contribution of SF_5CF_3 was lower and SF_6/SF_5CF_3 was highest (Fig. 6c). We anticipate that the spatial inhomogeneity observed for the two tracer gases also applies to odor contributions. However, the interaction of different odor sources into a mixed odor and the effects observed for dilution with distance are more complex and cannot be predicted with a simple additive approach. Furthermore, the differentiation of odors from biogas plants and animal husbandry is not feasible without excessive analytical efforts.

5. Conclusions and outlook

Our study validated an improved approach for odor impact assessment. The intensity of perceptible odor weighted by frequency demonstrated superior performance to odor frequency. This considered both weak and mixed odors and combined two odor dimensions: frequency and intensity. The spatial configuration of odor sources and tracer gas dosing, adjacent buildings, and local flow are relevant for the effective exposure level in the plume. By combining odor parameters, tracer gases with concentration and ratio, and wind direction even complex spatial interactions can be traced in terms of source. The source–tracer-related approach offers an improved odor impact assessment. These conclusions are based on the findings of this study. The decay of odor with distance along the longitudinal axis of the plume can be tracked systematically. A high agreement of the tracer gas concentrations with the parameters odor intensity weighted by frequency of intensity levels 1–6 OIF ($I \geq 1$) and odor frequency with intensity levels 3–6 OF ($I \geq 3$) on the impact side has been demonstrated. In a nested, homogeneous source configuration, the two tracer gases showed a perfect match, and the entire combined source was mapped exactly with just one tracer gas. Two spatially extended, separated odor and tracer sources depicted: (i) the partial decrease of the tracer concentration from the remote source already within the farm, (ii) the relevance of odor and tracer gas sources in close proximity to the individual positions of the plume, and (iii) the effect of the respective wind direction. Especially in combination with the prevailing wind direction, spatially extended sources, buildings, and their arrangements have a great bearing on odor impact in the surrounding area.

An outlook for advancing these findings may include a real-time display with the current local wind direction, which could further improve the optimal positioning of assessors in the plume. For nested sources, a reduction in survey efforts would be possible by focusing on the longitudinal plume axis. Since it is feasible to track odor sources based on the spatial arrangement via the concentration ratio of two tracer gases, such a combined source–tracer-related approach can be extended to track and assign more complex situations with odor nuisances on-site, for example, several odor sources, their arrangement, and contribution. These advances in odor impact assessment methods pave the way for greater confidence in onsite assessments as a basis for developing appropriate odor mitigation strategies.

CRediT authorship contribution statement

Margret Keck: Writing – review & editing, Writing – original draft, Visualization, Validation, Resources, Project administration, Methodology, Investigation, Funding acquisition, Formal analysis, Conceptualization. **Kerstin Zeyer:** Writing – original draft, Validation, Methodology, Investigation, Conceptualization. **Joachim Mohn:** Writing – review & editing, Writing – original draft, Resources, Methodology. **Sabine Schrade:** Writing – review & editing, Supervision, Resources, Project administration, Methodology, Investigation, Funding acquisition, Conceptualization.

Declaration of competing interest

The authors declare that they have no known competing financial interests or personal relationships that could have appeared to influence the work reported in this paper.

Acknowledgments

We would like to thank numerous people for their support, and help at Empa (L. Emmenegger), at Agroscope (T. Anken, M. Frei, M. Keller, B. Kürsteiner, K. Mager, M. Schick, M. Schlatter, B. Steiner, K. Weber), and the assessors for their sniffing work in field inspections; R. Wolz for proof reading; D. Herzog for creating graphics; and the two farmers who took part in the study for their precious cooperation. This project was co-supported by the Swiss Federal Office of Energy (SFOE), represented by S. Hermle [154356/103306, 2009].

Data availability

The data that has been used is confidential.

References

Aatamila, M., Verkasalo, P.K., Korhonen, M.J., Viluksela, M.K., Pasanen, K., Tiittanen, P., Nevalainen, A., 2010. Odor annoyance near waste treatment centers: A population-based study in Finland. J. Air Waste Manage. Assoc. 60, 412–418. https://doi.org/10.3155/1047-3289.60.4.412.

Al Jubori, M., 2016. Atmospheric modelling. Master of Science in Environmental Sanitation. Universiteit Gent, Belgium. https://lib.ugent.be/catalog/rug01:002275075.

Aubrun, S., Leitl, B., 2004. Unsteady characteristics of the dispersion process in the vicinity of a pig barn. Wind tunnel experiments and comparison with field data. Atmos. Environ. 38, 81–93. https://doi.org/10.1016/j.atmosenv.2003.09.039.

Bächlin, W., Rühling, A., Lohmeyer, A., 2002. Bereitstellung von Validierungsdaten für Geruchsausbreitungsmodelle – Naturmessung. Forschungsbericht FZKA-BWPLUS Förderkennzeichen BWE 20003. Ingenieurbüro Lohmeyer, Karlsruhe.

Barclay, J., Nietzsche Diaz, C., Shanahan, I., Trick, L., Bellasio, R., Tinarelli, G., Brusasca, G., Rosales, R., Galvin, G., Castelli, S.T., Balch, A., Romain, A.-C., Escoffier, C., Öttl, D., Duthier, E., Berbekar, E., Oliva, G., Schauberger, G., Hauschildt, H., Lauerbach, H., Arichábala, H., Guillot, J.-M., Hinderink, L., Yosef, O., Diosey, P., Prandl, R., Zarra, T., 2023. International Handbook on the Assessment of Odour Exposure Using Dispersion Modelling. AMIGO and OLORES.org, Spain. https://doi.org/10.5281/zenodo.8367724.

Barczak, R.J., Fisher, R.M., Wang, X., Stuetz, R.M., 2018. Variations of odorous VOCs detected by different assessors via gas chromatography coupled with mass spectrometry and olfactory detection port (ODP) system. Water Sci. Technol. 77, 759–765. https://doi.org/10.2166/wst.2017.569.

Berry, N.R., Zeyer, K., Emmenegger, L., Keck, M., 2005. Emissionen von Staub (PM10) und Ammoniak (NH3) aus traditionellen und neuen Stallsystemen mit Untersuchungen im Bereich der Mastschweinehaltung. Agroscope FAT Tänikon, Ettenhausen und Empa, Dübendorf.

Brattoli, M., de Gennaro, G., de Pinto, V., Loiotile, A.D., Lovascio, S., Penza, M., 2011. Odor detection methods: Olfactometry and chemical sensors. Sensors 11, 5290–5322. https://doi.org/10.3390/s110505290.

Bydder, C., Demetriou, J., 2019. Establishing the extent of odour plumes and buffers for waste handling facilities. Waste Manage 95, 356–364. https://doi.org/10.1016/j.wasman.2019.06.028.

Capelli, L., Sironi, S., Del Russo, R., Guillot, J.-M., 2013. Measuring odours in the environment vs. dispersion modelling: A review. Atmos. Environ. 79, 731–743. https://doi.org/10.1016/j.atmosenv.2013.07.029.

Davies, B.M., Jones, C.D., Manning, A.J., Thomson, D.J., 2000. Some field experiments on the interaction of plumes from two sources. Q. J. Roy. Meteor. Soc. 126, 1343–1366. https://doi.org/10.1002/qj.49712656508.

Eckhof, W., Gallmann, E., Grimm, E., Hartung, E., Kamp, M., Koch, R., Lang, M., Schauberger, G., Schmitzer, R., Sowa, A., 2012. Emissionen und Immissionen von Tierhaltungsanlagen – Handhabung der Richtlinie VDI 3894. KTBL-Schrift 494. Darmstadt.

EN 16841-1, 2016. Ambient air - Determination of odour in ambient air by using field inspection - Part 1: Grid method. European Committee for Standardization CEN, Brussels.

EN 16841-2, 2016. Ambient air - Determination of odour in ambient air by using field inspection - Part 2: Plume method. European Committee for Standardization CEN, Brussels.

Frechen, F.-B., 2000. Odour measurement and odour policy in Germany. Water Sci. Technol. 41 (6), 17–24. https://doi.org/10.2166/wst.2000.0088.

Freeman, T., Cudmore, R., 2002. Review of odour management in New Zealand. Air Quality Technical Report No. 24. Ministry for the Environment, Wellington, New Zealand.

Gostelow, P., Parsons, S.A., Stuetz, R.M., 2001. Odour measurements for sewage treatment works. Water Res 35, 579–597. https://doi.org/10.1016/S0043-1354(00)00313-4.

Gotow, N., Moritani, A., Hayakawa, Y., Akutagawa, A., Hashimoto, H., Kobayakawa, T., 2018. Effect of a warm-up sample on stabilizing the performance of untrained panelists in time–intensity evaluation. J. Sens. Stud. 33, e12309. https://doi.org/10.1111/joss.12309.

Griffiths, K.D., 2014. Disentangling the frequency and intensity dimensions of nuisance odour, and implications for jurisdictional odour impact criteria. Atmos. Environ. 90, 125–132. https://doi.org/10.1016/j.atmosenv.2014.03.022.

Hartmann, U., Grabowski, H.-G., 2011. Bewertung von Geruchsminderungsmassnahmen anhand der Geruchsstoffintensität. Gefahrstoffe – Reinhaltung der Luft 71 (10), 445–448.

Hawko, C., Verriele, M., Hucher, N., Crunaire, S., Leger, C., Locoge, N., Savary, G., 2021. A review of environmental odor quantification and qualification methods: The question of objectivity in sensory analysis. Sci. Total Environ. 795, 148862. https://doi.org/10.1016/j.scitotenv.2021.148862.

Hayes, J.E., Barczak, R.J., Suffet, I.M., Stuetz, R.M., 2023. The use of gas chromatography combined with chemical and sensory analysis to evaluate nuisance odours in the air and water environment. Environ. int. 180, 108214. https://doi.org/10.1016/j.envint.2023.108214.

Hayes, J.E., Stevenson, R.J., Stuetz, R.M., 2014. The impact of malodour on communities: A review of assessment techniques. Sci. Total Environ. 500–501, 395–407. https://doi.org/10.1016/j.scitotenv.2014.09.003.

Hove, C.Y., Van Langenhove, H., Van Weyenberg, S., Demeyer, P., 2016. Comparative odour measurements according to EN 13725 using pig house odour and n-butanol reference gas. Biosyst. Eng. 143, 119–127. https://doi.org/10.1016/j.biosystemseng.2016.01.002.

Hummel, T., Kobal, G., Gudziol, H., Mackay-Sim, A., 2007. Normative data for the "Sniffin' Sticks" including tests of odor identification, odor discrimination, and olfactory thresholds: an upgrade based on a group of more than 3,000 subjects. Eur. Arch. Oto-Rhino-L. 264, 237–243. https://doi.org/10.1007/s00405-006-0173-0.

Kaeppler, K., Mueller, F., 2013. Odor classification: A review of factors influencing perception-based odor arrangements. Chem. Senses 38, 189–209. https://doi.org/10.1093/chemse/bjs141.

Keck, M., Frei, M., Steiner, B., Schrade, S., 2018a. Synthesis of the attenuation of odour intensity with distance of cattle and pig husbandry as well as animal husbandry combined with biogas facilities. Chem. Eng. Trans. 68, 109–114. https://doi.org/10.3303/CET1868019.

Keck, M., Koutny, L., Schmidlin, A., Hilty, R., 2005. Odour in ambient air of pig housing systems with exercise yards and natural ventilation. Agrarforschung 12, 84–89. https://ira.agroscope.ch/de-CH/publication/37542.

Keck, M., Mager, K., Weber, K., Keller, M., Frei, M., Steiner, B., Schrade, S., 2018b. Odour impact from farms with animal husbandry and biogas facility. Sci. Total Environ. 645, 1432–1443. https://doi.org/10.1016/j.scitotenv.2018.07.182.

Keller, A., Hempstead, M., Gomez, I.A., Gilbert, A.N., Vosshall, L.B., 2012. An olfactory demography of a diverse metropolitan population. BMC Neurosci 13, 122. https://www.biomedcentral.com/1471-2202/13/122.

Koo, T.K., Li, M.Y., 2016. A guideline of selecting and reporting intraclass correlation coefficients for reliability research. J. Chiropr. Med. 15, 155–163. https://doi.org/10.1016/j.jcm.2016.02.012.

Laing, D.G., Francis, G.W., 1989. The capacity of humans to identify odors in mixtures. Physiol. Behav. 46, 809–814. https://doi.org/10.1016/0031-9384(89)90041-3.

Laor, Y., Parker, D., Pagé, T., 2014. Measurement, prediction, and monitoring of odors in the environment: a critical review. Rev. Chem. Eng. 30, 139–166. https://doi.org/10.1515/revce-2013-0026.

McGann, J.P., 2017. Poor human olfaction is a 19th-century myth. Science 356, eaam7263. https://doi.org/10.1126/science.aam7263.

Mohn, J., Zeyer, K., Keck, M., Keller, M., Zähner, M., Poteko, J., Emmenegger, L., Schrade, S., 2018. A dual tracer ratio method for comparative emission measurements in an experimental dairy housing. Atmos. Environ. 179, 12–22. https://doi.org/10.1016/j.atmosenv.2018.01.057.

Moldenhauer, A., Schädler, G., Rühling, A., Lohmeyer, A., 1999. Modellierung der Geruchs- und Ammoniakausbreitung aus Tierhaltungsanlagen im Nahbereich. Projekt 2191. Ingenieurbüro Lohmeyer, Karlsruhe, Dresden.

Nicell, J.A., 2009. Assessment and regulation of odour impacts. Atmos. Environ. 43, 196–206. https://doi.org/10.1016/j.atmosenv.2008.09.033.

Olesen, H.R., Løfstrøm, P., Berkowicz, R., Ketzel, M., 2005. Regulatory odour model development: Survey of modelling tools and datasets with focus on building effects. NERI Technical Report 541. National Environmental Research Institute, Denmark.

Pinheiro, J.C., Bates, D.M., 2000. Mixed-effects Models in S and S-Plus. Springer, New York. https://link.springer.com/book/10.1007/b98882.

R Core Team, R, 2023. A language and environment for statistical computing. R Foundation for Statistical Computing. http://www.r-project.org.

Schiffman, S.S., Bennett, J.L., Raymer, J.H., 2001. Quantification of odors and odorants from swine operations in North Carolina. Agr. Forest. Meteorol. 108, 213–240. https://doi.org/10.1016/S0168-1923(01)00239-8.

Schrade, S., Zeyer, K., Gygax, L., Emmenegger, L., Hartung, E., Keck, M., 2012. Ammonia emissions and emission factors of naturally ventilated dairy housing with solid floors and an outdoor exercise area in Switzerland. Atmos. Environ. 47, 183–194. https://doi.org/10.1016/j.atmosenv.2011.11.015.

Schürmann, G., 2007. Inverse Ausbreitungsmodellierung zur Emissionsratenbestimmung heterogener Flächenquellen. Diss. Universität Augsburg. https://d-nb.info/989390837/34.

Sucker, K., Both, R., Bischoff, M., Guski, R., Krämer, U., Winneke, G., 2008. Odor frequency and odor annoyance Part II: dose–response associations and their modification by hedonic tone. Int. Arch. Occup. Environ. Health 81, 683–694. https://doi.org/10.1007/s00420-007-0262-4.

Torrijos, M., 2016. State of development of biogas production in Europe. Procedia Environ. Sci. 35, 881–889. https://doi.org/10.1016/j.proenv.2016.07.043.

Van Langenhove, H., Van Broeck, G., 2001. Applicability of sniffing team observations: Experience of field measurements. Water Sci. Technol. 44, 65–70. https://doi.org/10.2166/wst.2001.0510.

VDI 3940-2, 2006. Measurement of odour impact by field inspection – Measurement of the impact frequency of recognizable odours: Plume measurement. VDI-Richtlinien, Beuth, Berlin.

VDI 3940-3, 2010. Measurement of odour impact by field inspection – Determination of odour intensity and hedonic odour tone. VDI-Richtlinien, Beuth, Berlin.

WMO, 2023. Guide to instruments and methods of observation – Measurement of meteorological variables, I. World Meteorological Organization, Geneva. WMO-No.8. https://library.wmo.int/idurl/4/68695.

Zhang, Q., Zhou, X., 2020. Assessing peak-to-mean ratios of odour intensity in the atmosphere near swine operations. Atmosphere 11, 224. https://doi.org/10.3390/atmos11030224.

Zorn, A., 2020. Key figures of the structural change of Swiss agriculture based on individual operational data. Agroscope Sci. 88, 1–58. https://doi.org/10.34776/as88g.